Ehrlich-Schwoebel barrier and interface-limited decay in island kinetics on Ag(100)

Xin Ge and Karina Morgenstern

*Leibniz Universität Hannover, Institut für Festkörperphysik, Abteilung für atomare und molekulare Strukturen (ATMOS),
Appelstr. 2, D-30167 Hannover, Germany*

We investigate diffusion and decay of adatom and vacancy islands on Ag(100) between ≈ 10 and ≈ 1000 nm^2 in size at room temperature by fast scanning tunneling microscopy. Adatom and vacancy islands decay in the diffusion and in the attachment limit, respectively. This adatom-driven kinetics confirms the existence of an Ehrlich-Schwoebel barrier on Ag(100). The dependence of the diffusivity of vacancy islands on island size is consistent with a kink-dominated periphery diffusion mechanism. Quantitative differences to previously published work are discussed.

I. INTRODUCTION

In surface science experiments, a metal surface is mostly cleaned by high-energy ion bombardment. Although the substrate is driven far from equilibrium during the ion erosion, its crystallinity is hardly affected.[1] The surface is then trapped in a variety of nonequilibrium configurations with a multitude of pits and mounds on the nanometer scale. Intelligent use of ion bombardment in combination with metal deposition opens the possibility to control nanoscale morphology. However, the created nanostructures are thermodynamically only metastable. Thus, the evolution of these structures into more stable structures is very important in order to ultimately produce controlled structures on the nanoscale. For example, on Ni(100), the exact amount of removed material affects crucially the post-treatment evolution of the structures.[2]

For an atomic-sale understanding of these processes, the coarsening of nanostructures has been followed in real time, some by low-energy electron microscopy (LEEM), e.g.,[3–5] but mostly by scanning tunneling microscopy (STM). STM research focused in particular on Cu and Ag surfaces and revealed fundamental concepts of island decay and diffusion.[6,7] Thereby, a nanocluster of monatomic height is called an adatom island, and a vacancy island is an agglomeration of missing adatoms within an otherwise crystalline layer. These systems are ideally suited for fundamental studies of coarsening of nanostructures in two dimensions. The most elementary kinetic processes are the decay of adatom and vacancy islands and their random motion over the surface. Surprisingly, the picture of Ag(100) is not yet complete with respect to these elementary processes. We thus return to this simple case, although, meanwhile, heteroepitaxial systems are at the focus of attention.[8–10]

In this paper, we investigate the decay of individual Ag adatom islands and vacancy islands on Ag(100). Adatom islands follow a decay as expected for adatom-driven decay in contrast to the expectation raised from ripening.[11] Vacancy islands decay linearly, indicative of a step-edge barrier. Furthermore, we compare the vacancy-island diffusion in dependence on island size to previously investigated adatom-island diffusivity. The smaller exponent found here as compared to (mainly) adatom-island diffusivity[12,13] is explained by the order-of-magnitude larger size range investigated here.

II. EXPERIMENTAL METHODS

Scanning tunneling microscopy (STM) measurements are performed with a variable temperature STM under ultrahigh vacuum (UHV) conditions (base pressure 2×10^{-10} mbar). A clean Ag(100) substrate is obtained by repeated cycles of Ne$^+$ sputtering and annealing. The sputtering is performed for 15 to 20 min at a partial neon pressure of $\approx 2.5 \times 10^{-5}$ mbar. The acceleration of the Ne$^+$ ions with 1.3 kV results in a sputtering current of 13 to 16 μA onto the sample and sample holder. This corresponds to between 3.6 and 4.4×10^{12} ions/(s mm^2) on the sample. The sample is then annealed for 10 to 15 min to approximately 950 K. Vacancy and adatom islands are produced by a 1 to 2 min sputter pulse after the last annealing at a partial neon pressure of $\approx 2 \times 10^{-5}$ mbar with an acceleration voltage of 500 V.

Changes to the structures are followed by repeatedly scanning the same spot of the surface at intervals between 20 and 30 s in constant current mode at room temperature. In total, almost 14 000 positions and sizes of vacancy islands and more than 2000 positions and sizes of adatom islands are analyzed. Special care is taken that the scanning process does not influence the evolution of structures and the analysis (cf. Ref. 14).

III. RESULTS AND DISCUSSION

Figure 1(a) shows a typical situation of the surface after 2 min of additional sputtering. Before this additional sputtering, three terraces were separated by double and triple steps. The image suggests that these have partly retracted and their position after sputtering is indicated by the arrows in the figure. On the three terraces, vacancy islands are created in the first three layers. In addition, there is one adatom island on the middle terrace, most probably a rest from a retracting terrace. Because of the energy that is necessary to create such steps, these structures are not in thermal equilibrium. We follow changes toward thermal equilibrium in time-lapse sequences, in which we repeatedly scan the same part of the surface at fixed time intervals. Figure 1(b) shows the same spot of the surface around 1.5 h later. The adatom island has decreased in size as have most vacancy islands, e.g., the one marked with "1."
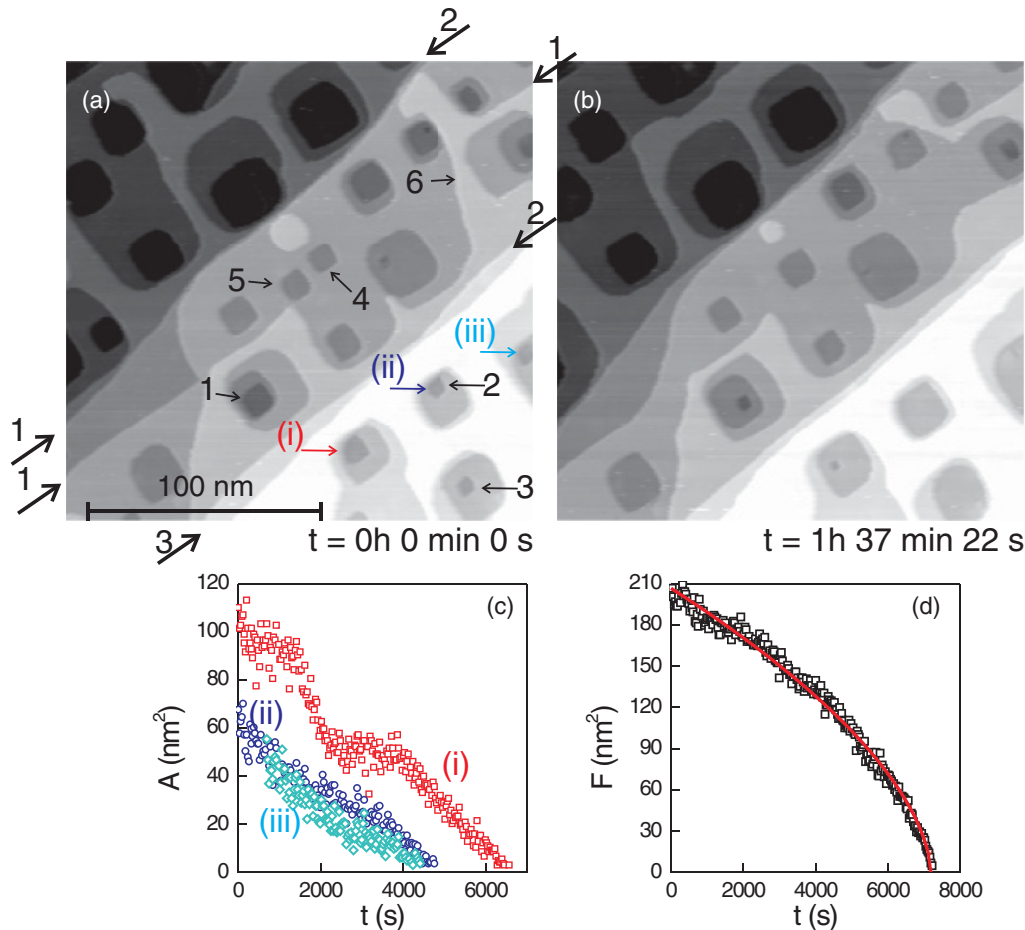
FIG. 1. (Color online) Large-scale STM image after sputtering for (a) 2 min and (b) same spot of the surface 1 h 37 min 22 s later; thick arrows in (a) point to pre-existing step edges: 1.12 nA, 1.03 V. (c) Area evolution of three vacancy islands from (a) and (b) as marked. (d) Area evolution of adatom island from (a) and (b); solid line is best fit of $y = a(t_0 - t)^\alpha$, yielding $a = (1.12 \pm 0.06)$ nm^2/s, $b = (7192 \pm 15)$ s, and $\alpha = 0.59 \pm 0.01$.

Some vacancy islands have disappeared completely, e.g., "2" and "3." A pair of vacancy islands ("4","5") has coalesced to form a larger vacancy island, indicative of a motion of the vacancy islands. Finally, a small bridge "6" has retracted.

The decay of some of the vacancy islands and of the adatom island are displayed in Figs. 1(c) and 1(d), respectively. The decay behavior differs qualitatively between the two types of islands and quantitatively between the different vacancy islands. The adatom island decays faster, the smaller it is, while the vacancy islands decay almost linearly in time. The decay rate of the largest of the vacancy islands in Fig. 1(c) (red squares) shows a steplike behavior with alternating regions of slow and fast decay. The separate regions are all consistent with a linear decay. These differences are discussed in the following sections.

A. Decay of adatom islands

1. Introduction

In standard theory, the changes in island size are explained based on the behavior of individual adatoms.[6,7] The change of the island area is determined by the transfer of such atoms from the step edge onto the terrace, the transport of the adatoms

away from their position close to the step edges to sinks, and an attachment of the adatoms to these sinks (usually other step edges). Depending on which of the processes is rate limiting, the island's decay is named either diffusion limited or detachment-attachment limited. The latter is sometimes also called interface limited. The two limiting cases can be discriminated by following the decay rate of individual islands in time. The island area A should follow

$$A \propto (t_0 - t)^\alpha \qquad (1)$$

with t_0 the time, at which the island is completely decayed, and the exponent α depending on the type of decay. Values of $\alpha \approx 2/3$ and $\alpha \approx 1$ are indicative for diffusion-limited decay and interface-limited decay, respectively. Certain assumptions in solving the diffusion equations (see below) in order to derive Eq. (1) are not fulfilled for the smallest islands observed in STM and, thus, the effectively measured exponents are somewhat larger than 1 and somewhat smaller than 2/3, respectively.[15]

2. Results

The exponent determined for the adatom island shown in Fig. 1(d) points with $\alpha = 0.59$ clearly to diffusion-limited
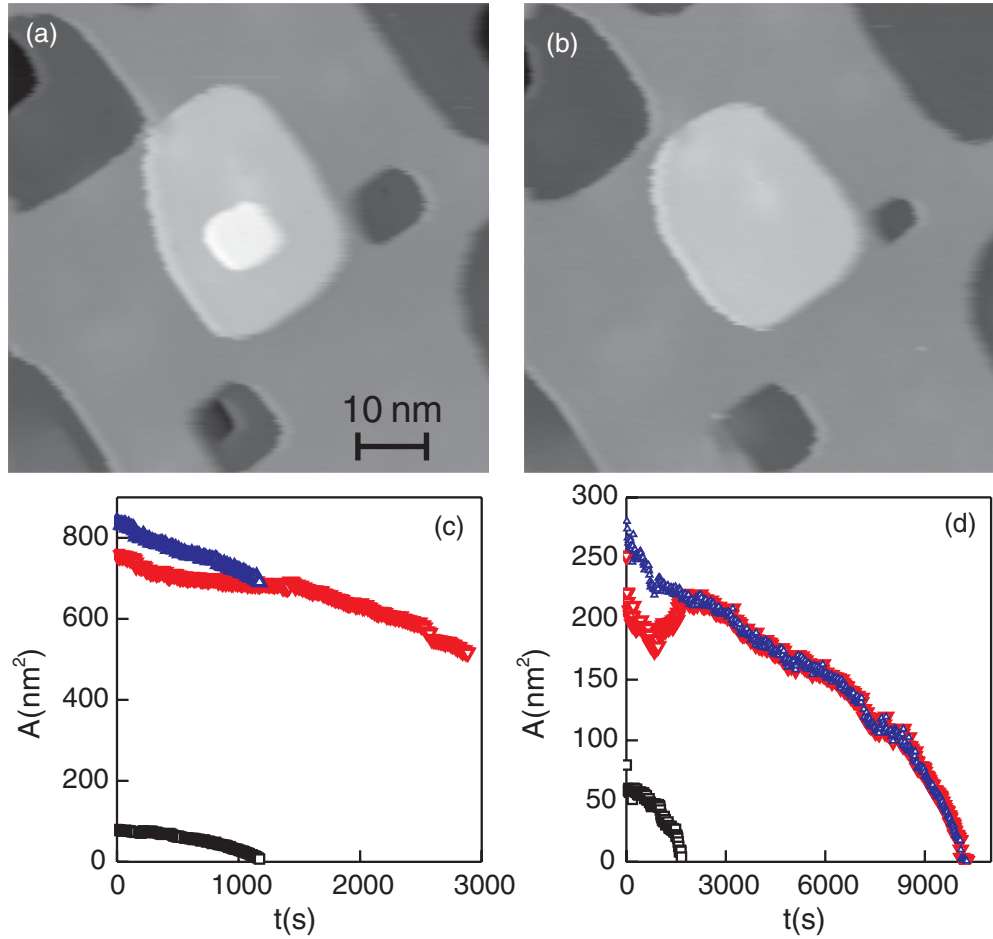
FIG. 2. (Color online) Decay of adatom islands: (a), (b) Snapshots from a movie of an adatom island situated on top of another larger one: $\Delta_{a,b}$ t = 17 min 44 s, 0.86 nA, 0.713 V. (c) Time evolution of adatom islands from (a) black squares: upper adatom island; red down triangles: lower adatom island; blue up triangles: sum of both. (d) Time evolution for a different pair of adatom islands, same color coding.

decay. We discuss the adatom-island decay further on the evolution of a two-layer adatom-island stack (Fig. 2). This geometry excludes a strong influence of the immediate surrounding on the decay for the upper adatom islands, which is usually observed in diffusion-limited ripening.[16] Within roughly 18 min, the upper adatom island in Figs. 2(a) and 2(b) decays completely. As shown in Fig. 2(c), the decay of this adatom island slows down the decay of the adatom island in the second layer. The rate of loss increases after the complete decay of the upper adatom island. In the second example in Fig. 2(d), the adatom island in the second layer even grows during the decay of the top-layer adatom island. In total, the stack loses atoms. This loss is continued after the complete decay of the upper adatom island.

Clearly, all adatom islands decay faster than linear, indicative of the diffusion-limited behavior. A quantitative analysis of a larger number of adatom islands yields a decay exponent of $\alpha = (0.54 \pm 0.03)$. This value is smaller than the 2/3 expected for the diffusion-limited decay of large adatom islands. As shown before for adatom-island decay on Ag(111),[15] the approximations employed to derive this exponent from the diffusion equations are not valid for small islands and, strictly speaking, the exponent is not a physical quantity to describe the decay for the smallest islands investigated here. Nonetheless,

it is useful to compare the apparent exponent for different systems. The apparent exponent determined for Ag(111) of 0.54 ± 0.10 for adatom islands in the same size range is very much the same as the effective exponent determined here.

Note that this decay behavior results from the Gibbs-Thomson relation that predicts that the adatom density ρ_{ad} depends exponentially on curvature $1/r$ according to

$$\rho_{ad} = \rho_{\infty} e^{\gamma/kTnr} \tag{2}$$

with some parameters that depend on the surface: γ is the free step energy, n is the atomic density in the surface layer, and ρ_{∞} is the equilibrium adatom density in front of a straight step. Thus, the flow of atoms from an island to the terrace is larger the smaller the island. We conclude that adatom islands of Ag/Ag(100) show diffusion-limited decay driven by adatoms.

B. Decay of vacancy islands

For the investigation of vacancy islands, we take the same approach as for the decay of adatom islands. A stack of two vacancy islands is shown in Figs. 3(a) to 3(e). As long as the smaller vacancy island decays, the larger vacancy island grows. The whole stack loses vacancies, and this loss is continued after the complete filling of the smaller vacancy island. As also
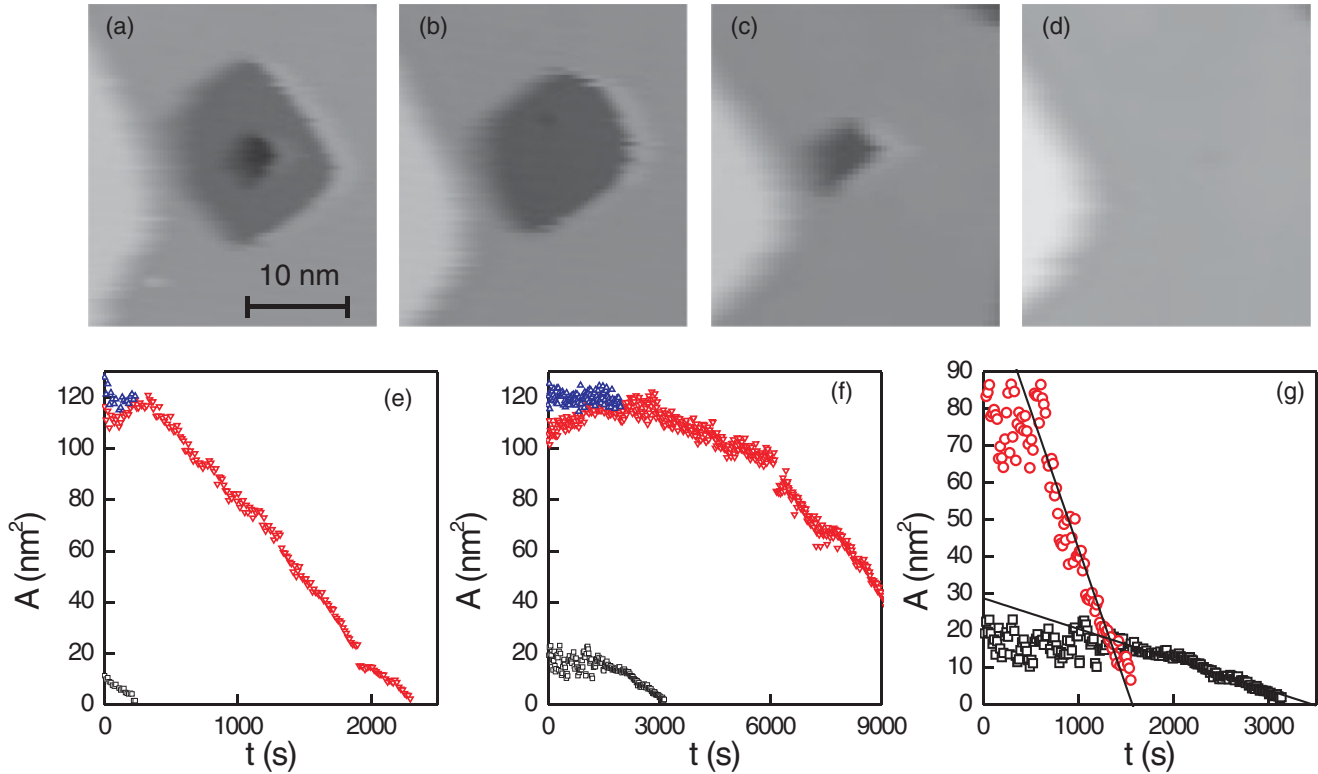
FIG. 3. (Color online) Decay of vacancy islands: (a)–(d) Snapshots of a time-lapse series showing a vacancy island situated within a larger vacancy island: 0.86 nA, 0.713 V, $\Delta t_{a,b} = 10$ min 5 s, $\Delta t_{b,c} = 21$ min 46 s, $\Delta t_{c,d} = 12$ min 3 s. (e) Time evolution of vacancy islands in (a); black squares: lower vacancy island; red down triangles: upper vacancy islands; blue up triangles: sum. (f) Time evolution of a different set of vacancy islands with same color coding. (g) Decay of two vacancy islands in the same layer but well separated.

observable in the second example in Fig. 3(f), material from the larger surrounding vacancy island fills the inner vacancy island.

Despite the steps in the decay in some of the vacancy islands [Fig. 1(c)], the overall decay of the vacancy islands in their final decay is linear. For the final decay of a large number of vacancy islands, an exponent of 1.02 ± 0.05 is determined. The decay of the vacancy islands is thus interface limited.

We now return to the different decay rates observed in Fig. 1(c). Not only are vacancy islands seen to decay at different rates in time, but the decay rate depends also on their exact position on the terrace. The two vacancy islands shown in Fig. 3(g) are situated in the same layer and are imaged simultaneously. Both vacancy islands decay linearly, but their decay rate differs by one order of magnitude. The effect of different decay rates is thus a local effect. However, under equilibrium conditions, a constant decay rate independent of environment is expected for interface-limited decay.[6,7]

In order to understand the influence of the environment, we shortly recapitulate some essential part of the reasoning that leads to the area dependence in Eq. (1). In the theoretical description of the interface-limited decay, the adatom density on the terrace is assumed to be constant for a given temperature. This density determines the number of adatoms impinging onto the vacancy island and thus the filling rate. For a terrace that is limited by straight steps, this adatom density is ρ_∞. However, for a terrace that is limited by curved steps, the

Gibbs-Thomson relation predicts that the adatom density ρ_{ad} depends exponentially on curvature $1/r$ (see above). In deriving Eq. (1), the surrounding is described by a large vacancy island of curvature $-1/R$, which is so large that the exponential is linearized to give a factor of "1" only. This is an oversimplification for the present situation. Moreover, in the example of Fig. 1(a), the adatom island and the connection "6" enhance the adatom density locally. The locally enhanced adatom density in turn increases the vacancy-island decay rate. In fact, the decay rate of the vacancy islands close to these two structures is enhanced.

The effect of a local enhancement of adatoms on the vacancy-island decay rate is directly demonstrated in Fig. 4 for a vacancy island, for which the environment changes abruptly due to coalescence of the surrounding vacancy island with a neighboring one. The vacancy decay accelerates considerably after this coalescence, as shown in Figs. 4(a) to 4(c). Such a coalescence leads to necks of high curvature, which enhance the adatom-island density locally [c.f. Eq. (2)] so that it is larger than the equilibrium density at the current temperature.[17] A second example of such coalescence increased decay rate is presented in Fig. 4(d). The decay rate increases by two orders of magnitude. This corresponds to a rate expected at a 20% higher temperature, i.e., around 360 K. We conclude that the vacancy-island decay on Ag(100) is interface limited, but depends nonetheless on the local adatom concentration.
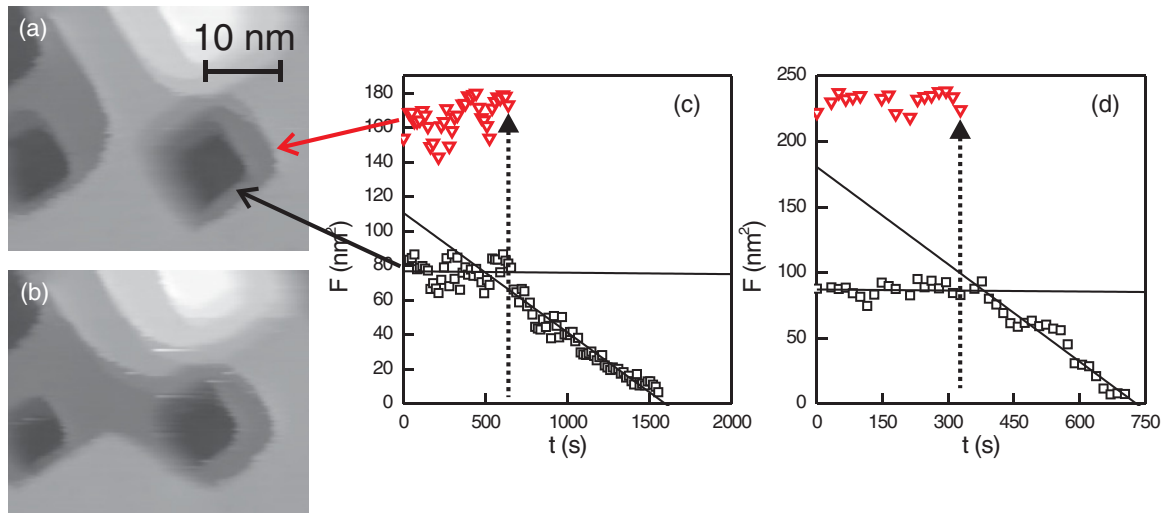
FIG. 4. (Color online) Influence of surrounding on vacancy-island decay: (a), (b) Snapshots of two vacancy islands that coalesce during the decay of vacancy islands in the next deeper layer: 0.3 nA, 1 V, $\Delta t_{a,b} = 5$ min 10 s. (c), (d) Time evolution of vacancy island in deeper layer (squares) surrounded originally by a vacancy island with the size shown as down triangles; the larger vacancy island in the upper layer coalesces with a neighboring vacancy island at the respective arrow.

C. Discussion of island decay

We compare the observed decay behavior to island decay within other homoepitaxial systems of noble metals. On the Cu(100) surface, the adatom-island decay is linear in time, i.e., interface limited at room temperature[18] and between 343 and 413 K.[18] This is not expected for adatom-driven decay in a homoepitaxial system. It was proposed that the decay is not mediated by adatoms but by vacancies.[18,19] Theory supported that the diffusion of vacancies on Cu(100) is lower in energy than that of adatoms.[20]

For Ag(100), the decay of individual islands has not yet been investigated. Instead, the ripening within larger adatom-island ensembles was investigated.[21] It is expected that diffusion-driven ensembles rather coarsen via Ostwald ripening, i.e., larger islands grow at the expense of smaller islands, while interface-driven ensembles coarsen via Smolouchowski ripening, i.e., islands diffuse and coalesce.[22] As Ostwald ripening was observed,[21] the decay of Ag adatom islands on Ag(100) should be diffusion limited. However, in a following study,[11] adatom-island agglomerations on Ag(100) up to 0.65 nm were found to coarsen at room temperature via Smolouchowski ripening, i.e., via diffusion of the adatom islands and subsequent coalescence. Vacancy islands coarsened via Ostwald ripening. The latter study thus pointed to a vacancy-mediated decay.

Here, the determined exponents imply that the adatom-island decay on Ag(100) is diffusion limited, but the vacancy-island decay is interface limited. We thus confirm the earlier study,[21] which predicted diffusion-limited decay for adatoms and thus a kinetics driven by adatoms. The observed dependence of the vacancy-island decay rate on adatom density is a further strong indication for a mainly adatom-mediated kinetics. This shows that the type of decay is difficult to predict from ripening studies.

The same kind of behavior as for Ag(100) was found for both adatom islands and vacancy islands on Ag(111).[15]

Thus, Ag(100) is more similar to Ag(111) and distinctly different from the one on Cu(100), or more broadly speaking, material is more important than face (at least in this particular case).

The observed different decay behavior for adatom and vacancy islands in this homoepitaxial system furthermore implies a step-edge barrier for adatoms to fill the vacancy islands.[6,7] This so-called Ehrlich-Schwoebel barrier[23,24] has been established for Ag(111) first in growth experiments[25,26] and later in decay measurements,[27] equivalent to the approach here. It is, however, much debated for the Ag(100) face. Early density functional theory (DFT) calculated a negligible difference between the hopping diffusion of Ag on the terrace and the exchange diffusion of it over the close-packed ⟨110⟩ step edge.[28] For the more open ⟨100⟩ edge, even a negative Ehrlich-Schwoebel barrier was proposed.[29] More recent DFT calculations yielded a positive barrier of 20 meV.[30] Experimentally, temperature-dependent growth experiments revealed a small positive average step-edge barrier of (30 ± 5) meV (Ref. [31]) and a barrier of 60 to 70 meV for the close-packed edge in a later analysis of the same group.[32] Our different experimental approach confirms the existence of a positive ES barrier.

D. Vacancy-island diffusion

1. Introduction

We now turn to the diffusion of the islands. For diffusion of homoepitaxial islands, it is generally assumed that the displacement of individual island atoms leads to a center-of-mass displacement of the islands as a whole.[6,7] On a surface, it is imaginable that the individual adatoms perform a random motion along the island boundary. This is called periphery diffusion. Alternatively, the adatoms may detach to the terrace, perform a random motion over this terrace, and then reattach at a different part of the island. This is called terrace diffusion.

For these two scenarios, simple power-law dependencies were proposed originally:

$$D \propto A^{-\beta} \qquad (3)$$

with D the island's diffusivity and A the island's area. An exponent of $\beta = 1.0$ should indicate terrace diffusion and one of $\beta = 1.5$ periphery diffusion.[33] However, for periphery diffusion, the originally assumed isotropic motion of the adatom along the island's periphery is too simplistic.[12] It is more realistic to assume that the adatoms alternately move slower from kink sites and faster along straight edges. For the case of Ag adatom islands on Ag(100), this was modeled theoretically.[12] The exponent smoothly varies between 0.5 and 1.5 in dependence on the average separation between kinks along the boundary,[12] i.e., the exact value is related to the roughness of the step edge. A noninteger exponent is thus indicative of periphery diffusion along a faceted periphery.

Indeed, the periphery-driven diffusion of adatom islands on Cu(100) and Ag(100) yielded noninteger exponents with $\beta = 1.14$ for Ag and $\beta = 1.25$ for Cu. Likewise, noninteger exponents of (1.33 ± 0.11) and (1.4 ± 0.1) were measured for the (111) faces of Ag and Cu, respectively.[34]

Only limited data are available for diffusion of vacancy islands on Ag(100).[35] The data are consistent with an equal diffusion coefficient for adatoms and vacancy islands with a scaling of 1.15 in the size range between 8 and 80 nm^2.

2. Results

We here concentrate on the vacancy-island diffusion for a much larger size range than previously investigated in island-diffusion studies by STM.[12–14,21,34] We explore the diffusivity in dependence of vacancy-island size for vacancy islands between 3 and 1670 nm^2. In time-lapse series recorded between images as shown in Figs. 1(a) and 1(b), we determine the relative position of the vacancy islands. One example is shown in Fig. 5(a).

The diffusivity D is calculated from the mean-square displacements $\langle \Delta x \rangle^2$ and $\langle \Delta y \rangle^2$ in the two scanning distances according to the Einstein relation $\langle \Delta x \rangle^2 = 2D\Delta t$ with Δt the time lapse between the images. In order to reduce effects of thermal drift, we measure the relative motion of an island either with respect to an immobile defect or with respect to another island of similar size. In the latter case, the thus determined diffusivity is just twice that of a single island ($D_{2\text{vac}} = D_1 + D_2$). For the example in Fig. 5(a), the distance distribution is clearly Gaussian [Fig. 5(b)]. Thus, the motion is random and not hindered in any direction.

As the vacancy islands decay during the motion, we separate each vacancy island in size classes. We adapt these classes such that each of the values shown in the diffusivity plot in Fig. 5(c) is based on at least 400 data points. In the double-logarithmic plot, the diffusivities for the different vacancy-island sizes clearly fall on one line. The data points show a simple power-law dependence with an exponent of $\beta = 0.76 \pm 0.16$, indicative of periphery diffusion.

3. Discussion of vacancy-island diffusion

The exponent of $\beta = 0.76$ is considerably smaller than the $\beta = 1.14$ observed for adatom islands on the same surface in previous studies.[12,21] We discuss different scenarios to explain this discrepancy. First, our exponent varies slightly for different grouping of the data, i.e., for different size classes. However, a mean value larger than 0.81 was not achievable even under extreme choices.

We next controlled whether the different type of island is responsible for this deviation. Although the statistics of the adatom islands is somewhat smaller, their diffusivities fall on the same line as that of the vacancy islands [Fig. 5(c), small dots].

Finally, we sketch in the same graph the diffusivity in dependence of island area determined previously for adatom islands in Ref. 12 [green line in Fig. 5(b)]. This quantitative comparison shows that this previous dependency is very close to the values determined here in the same size range. This suggests that the difference might simply be due to the limited size range in previous STM studies and the error bar given there might have been somewhat optimistic. Even in our study, the determination of the prefactor is rather uncertain with a large
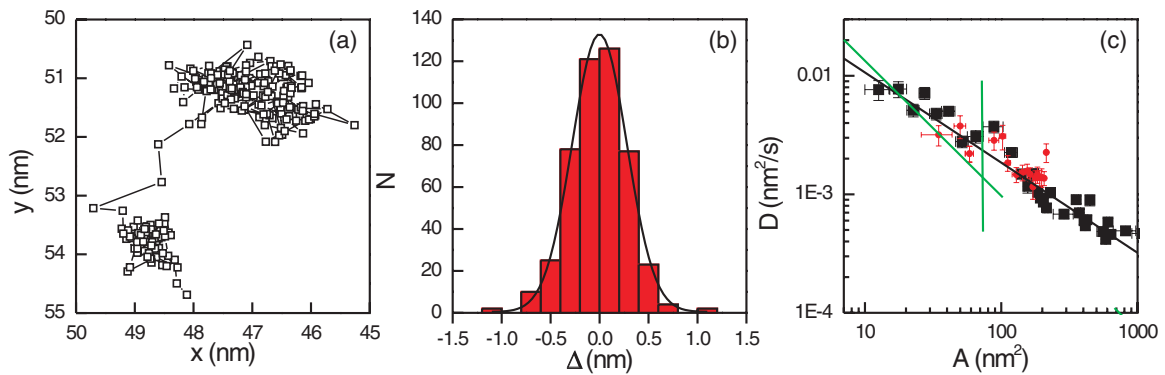

FIG. 5. (Color online) Diffusion of vacancy islands: (a) Example of the relative motion of two vacancy islands with areas of 225 and 216 nm^2 imaged roughly 250 times at intervals of ≈ 29 s. (b) Distribution of distances Δ in either x or y for motion shown in (a). (c) Diffusivity D in dependence of island area A; vacancy islands (black squares) and adatom islands (red circles); black line is fit to vacancy island data yielding $D_0 = (6.16 \pm 5.01) \times 10^{-2}$ nm^2/s and $\beta = 0.761 \pm 0.156$; green (gray) line is fit of adatom-island diffusivities measured by Ref. 12 within the adatom-island range up to 73 nm^2 as marked by vertical line; for the latter, $D_0 = (0.185 \pm 0.045)$ nm^2/s and $\beta = 1.14 \pm 0.05$ (Ref. 12).

error bar, although covering an 80% larger size range than the previous studies.

Theory has determined the diffusivity exponent based on the surface-embedded-atom method for adatom islands consisting of 100 to 1000 atoms, which corresponds to 8.3 to 83 nm^2.[36] The adatom-island motion is 99% due to adatoms diffusing around the periphery of the adatom islands because of the low energy for this diffusion of only 0.11 eV. The exponent decreases from 1.49 and 1.205 in the investigated size range. We do not see any specific change in exponent with vacancy-island size in this range or for our much larger size range. This might be obstructed in the scattering of the data.

IV. CONCLUSION

We have investigated island kinetics on Ag(100). The adatom islands decay in the diffusion limit and the vacancy islands decay in the interface limit. This is strong experimental evidence for an Ehrlich-Schwoebel barrier on Ag(100). Both decays are driven by adatoms in contrast to decay on Cu(100). Furthermore, we demonstrated the importance of the immediate surrounding in interface-limited decay, a fact that is usually ignored. Concerning diffusion studies, we demonstrated that a large size range of at least two orders of magnitude is necessary for a reliable determination of the diffusion exponent.

Our study shows that a simple transfer of results from a similar surface of same symmetry [here Cu(100) to Ag(100)] as well as from adatom islands to vacancy islands is not feasible for decay and diffusion of islands, respectively. It is thus indispensable to study each system of interest individually in order to establish an extensive database for the future control of nanoscale morphology.

[1]Ch. Teichert, Ch. Ammer, and M. Klaua, Phys. Status Solidi A **146**, 223 (1994).

[2]M. S. Hoogemann, M. A. J. Klik, R. van Gastel, and J. W. M. Frenken, J. Phys.: Condens. Matter **11**, 4349 (1999).

[3]W. Theis, N. C. Bartelt, and R. M. Tromp, Phys. Rev. Lett. **75**, 3328 (1995).

[4]N. C. Bartelt, W. Theis, and R. M. Tromp, Phys. Rev. B **54**, 11741 (1996).

[5]H. Hibino, C.-W. Hu, T. Ogino, and I. S. T. Tsong, Phys. Rev. B **63**, 245402 (2001).

[6]M. Giesen, Prog. Surf. Sci. **68**, 1 (2001).

[7]K. Morgenstern, Phys. Status Solidi B **242**, 773 (2005).

[8]Y. Han, B. Unal, F. Qin, D. Jing, C. J. Jenks, D.-J. Liu, P. A. Thiel, and J. W. Evans, Phys. Rev. Lett. **100**, 116105 (2008).

[9]C. T. Campbell, S. C. Parker, and D. E. Starr, Science **298**, 811 (2002).

[10]C. Zaum, M. Rieger, K. Reuter, and K. Morgenstern, Phys. Rev. Lett. **107**, 046101 (2011).

[11]J.-M. Wen, J. W. Evans, M. C. Bartelt, J. W. Burnett, and P. A. Thiel, Phys. Rev. Lett. **76**, 652 (1996).

[12]W. W. Pai, A. K. Swan, Z. Zhang, and J. F. Wendelken, Phys. Rev. Lett. **79**, 3210 (1997).

[13]P. A. Thiel, M. Shen, D.-J. Liu, and J. W. Evans, J. Phys. Chem. C **113**, 5047 (2009).

[14]K. Morgenstern, G. Rosenfeld, B. Poelsema, and G. Comsa, Surf. Sci. **352-354**, 956 (1996).

[15]K. Morgenstern, G. Rosenfeld, and G. Comsa, Phys. Rev. Lett. **76**, 2113 (1996).

[16]K. Morgenstern, G. Rosenfeld, and G. Comsa, Surf. Sci. **441**, 289 (1999).

[17]M. Eßer, K. Morgenstern, G. Rosenfeld, and G. Comsa, Surf. Sci. **402-404**, 341 (1998).

[18]J. B. Hannon, C. Klünker, M. Giesen, H. Ibach, N. C. Bartelt, and J. C. Hamilton, Phys. Rev. Lett. **79**, 2506 (1997).

[19]C. Klünker, J. B. Hannon, M. Giesen, H. Ibach, G. Boisvert, and L. J. Lewis, Phys. Rev. B **58**, R7556 (1998).

[20]G. Boisvert and L. J. Lewis, Phys. Rev. B **56**, 7643 (1997).

[21]J.-M. Wen, S.-L. Chang, J. W. Burnett, J. W. Evans, and P. A. Thiel, Phys. Rev. Lett. **73**, 2591 (1994).

[22]G. Rosenfeld, K. Morgenstern, I. Beckmann, W. Wulfhekel, E. Lægsgaard, F. Besenbacher, and G. Comsa, Surf. Sci. **402-404**, 401 (1998).

[23]R. L. Schwoebel and E. J. Shipsey, J. Appl. Phys. **37**, 3682 (1966); R. L. Schwoebel, *ibid.* **40**, 614 (1969).

[24]G. Ehrlich and F. G. Hudda, J. Chem. Phys. **44**, 1039 (1966).

[25]K. Bromann, H. Brune, H. Röder, and K. Kern, Phys. Rev. Lett. **75**, 677 (1995).

[26]J. A. Meyer, J. Vrijmoeth, H. A. van der Vegt, E. Vlieg, and R. J. Behm, Phys. Rev. B **51**, 14790 (1995).

[27]K. Morgenstern, G. Rosenfeld, E. Lægsgaard, F. Besenbacher, and G. Comsa, Phys. Rev. Lett. **80**, 556 (1998).

[28]B. D. Yu and M. Scheffler, Phys. Rev. Lett. **77**, 1095 (1996).

[29]U. Kürpick and T. S. Rahman, Phys. Rev. B **57**, 2482 (1998).

[30]H. Yildirim and T. S. Rahman, Phys. Rev. B **80**, 235413 (2009).

[31]C. R. Stoldt, K. J. Caspersen, M. C. Bartelt, C. J. Jenks, J. W. Evans, and P. A. Thiel, Phys. Rev. Lett. **85**, 800 (2000).

[32]K. J. Caspersen, C. R. Stoldt, A. R. Layson, M. C. Bartelt, P. A. Thiel, and J. W. Evans, Phys. Rev. B **63**, 085401 (2001).

[33]S. V. Khare and T. L. Einstein, Phys. Rev. B **54**, 11752 (1996).

[34]D. C. Schlößer, K. Morgenstern, L. K. Verheij, G. Rosenfeld, F. Besenbacher, and G. Comsa, Surf. Sci. **465**, 19 (2000).

[35]M. Shen, J.-M. Wen, C. J. Jenks, P. A. Thiel, D.-J. Liu, and J. W. Evans, Phys. Rev. B **75**, 245409 (2007).

[36]M. I. Haftel, Phys. Rev. B **64**, 125415 (2001).